## Supplementary Materials:

**Table S1: Real-time PCR primer sequences used in this study**

| Gene | Forward primer (5' to 3') | Reverse primer (3' to 5') |
|---|---|---|
| *RAT-TNF-α* | CCGAGATGTGGAACTGGCAGAG | CCACGAGCAGGAATGAGAAGAGG |
| *RAT-IL-1β* | TCTCACAGCAGCATCTCGACAAG | CCACGGGCAAGACATAGGTAGC |
| *RAT-GM-CSF* | GATGCCGCTTGTCAGTGCTAAC | GGTCGTAATGCTGCTGCCTATTG |
| *RAT-GAPDH* | ACGGCAAGTTCAACGGCACAG | CGACATACTCAGCACCAGCATCAC |
| *MOU- GAPDH* | GGCAAATTCAACGGCACAGTCAAG | TCGCTCCTGGAAGATGGTGATGG |
| *MOU-COL2A1* | ACGAGGCAGACAGTACCTTGAG | TGGTTGTTCAGTGACTTGAGTGTAG |
| *MOU-COLX* | GATGCCGCTTGTCAGTGCTAAC | GGTCGTAATGCTGCTGCCTATTG |
| *MOU-MMP13* | CAGTTGACAGGCTCCGAGAAATG | CACATCAGGCACTCCACATCTTG |
| *MOU-ACAN* | TCCGACATAGACACAGGCACTTC | GCTGATGGCAACATTCACCTCTG |
| *MOU-ADAMTS5* | GCTCCTCTTGGTGGCTGACTC | GGCGGATGTGGTTCTCAATGC |
| *MOU- IL-6* | GGCTAAGGACCAAGACCATCC | GCACTAGGTTTGCCGAGTAGA |
| *MOU-STAT1* | GCCTCTCATTGTCACCGAAGAAC | TGGCTGACGTTGGAGATCACCA |
| *MOU- CCL2* | GCTACAAGAGGATCACCAGCAG | GTCTGGACCCATTCCTTCTTGG |
| *MOU- CCL24* | ATTCCAGAAAACCGAGTGGTTAGC | GCATCCAGTTTTTGTATGTGCCTC |
| *MOU- CCL8* | GGGTGCTGAAAAGCTACGAGAG | GGATCTCCATGTACTCACTGACC |

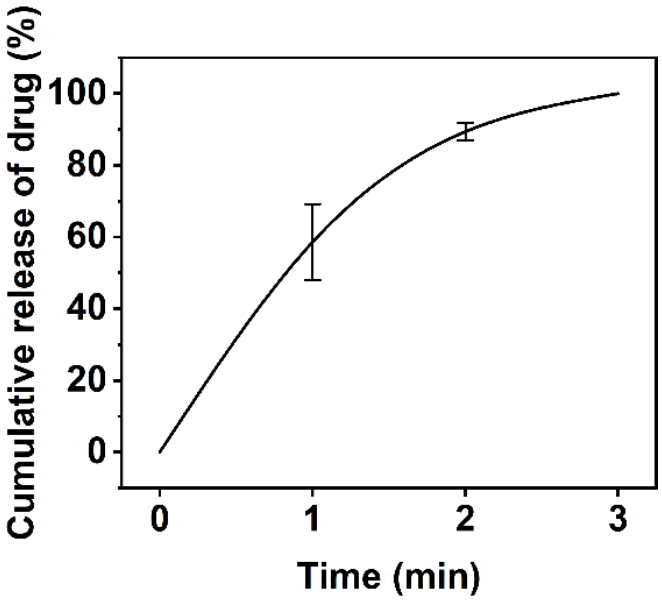


**Figure S1:** The cumulative release curve of FITC-labeled BSA from PVP MNs following immersion in water.

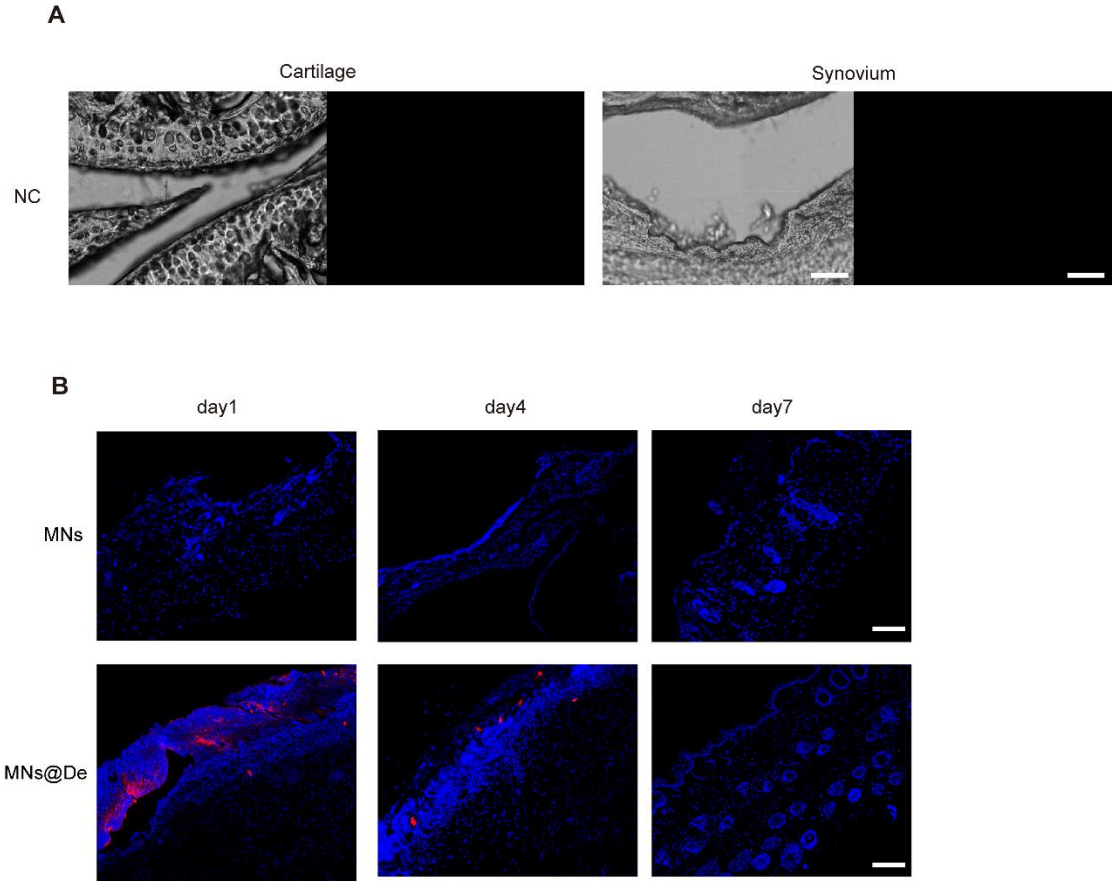


**Figure S2: The drug diffusion of MNs@De in the skin surface of the knee joint.**

(A) Negative control group for confocal fluorescence imaging. (B) Fluorescence images of the blank microneedle group and the MNs@De group on the skin surface of the knee joint, with blue representing DAPI and red representing Cy5.5-labelled denosumab. Scale bars, 100 μm.

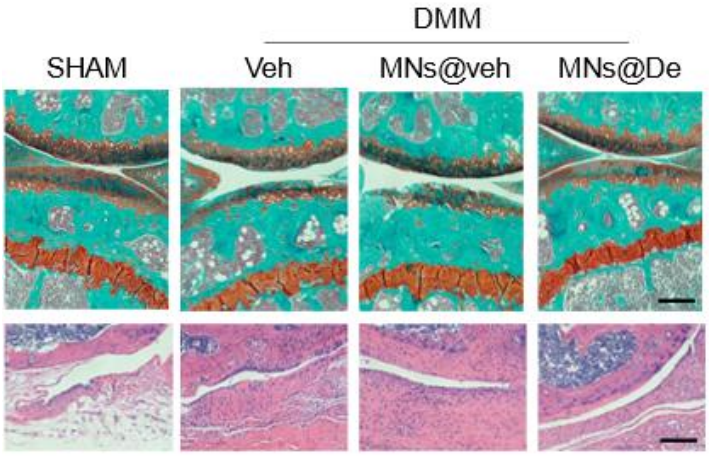


**Figure S3:**Examples of Safranin O and H&E staining in SHAM, DMM, DMM+MNs@veh, DMM+MNs@De mice. Scar bar,200um.

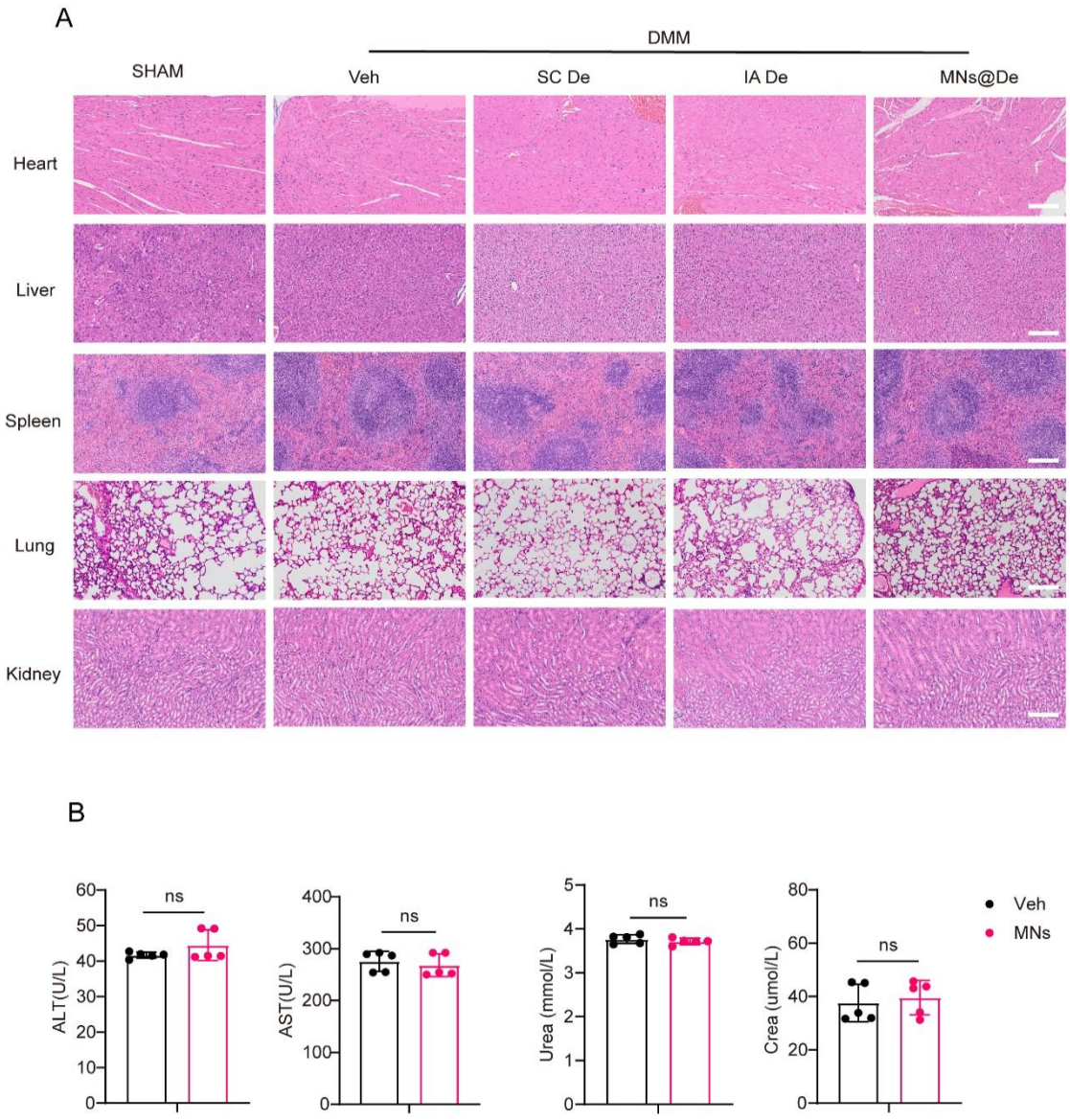


**Figure S4: Microneedle toxicity testing on major organs of mice.**

(A) H&E staining of organs(heart, liver, spleen, lung, kidney) in sham,dmm,SC De, IA De and MNs@De mice. Scar bar, 100um. (B) Detection of liver and kidney function indicators (ALT, AST, Urea, Crea) in Veh and MNs mice. (n = 5 per group).

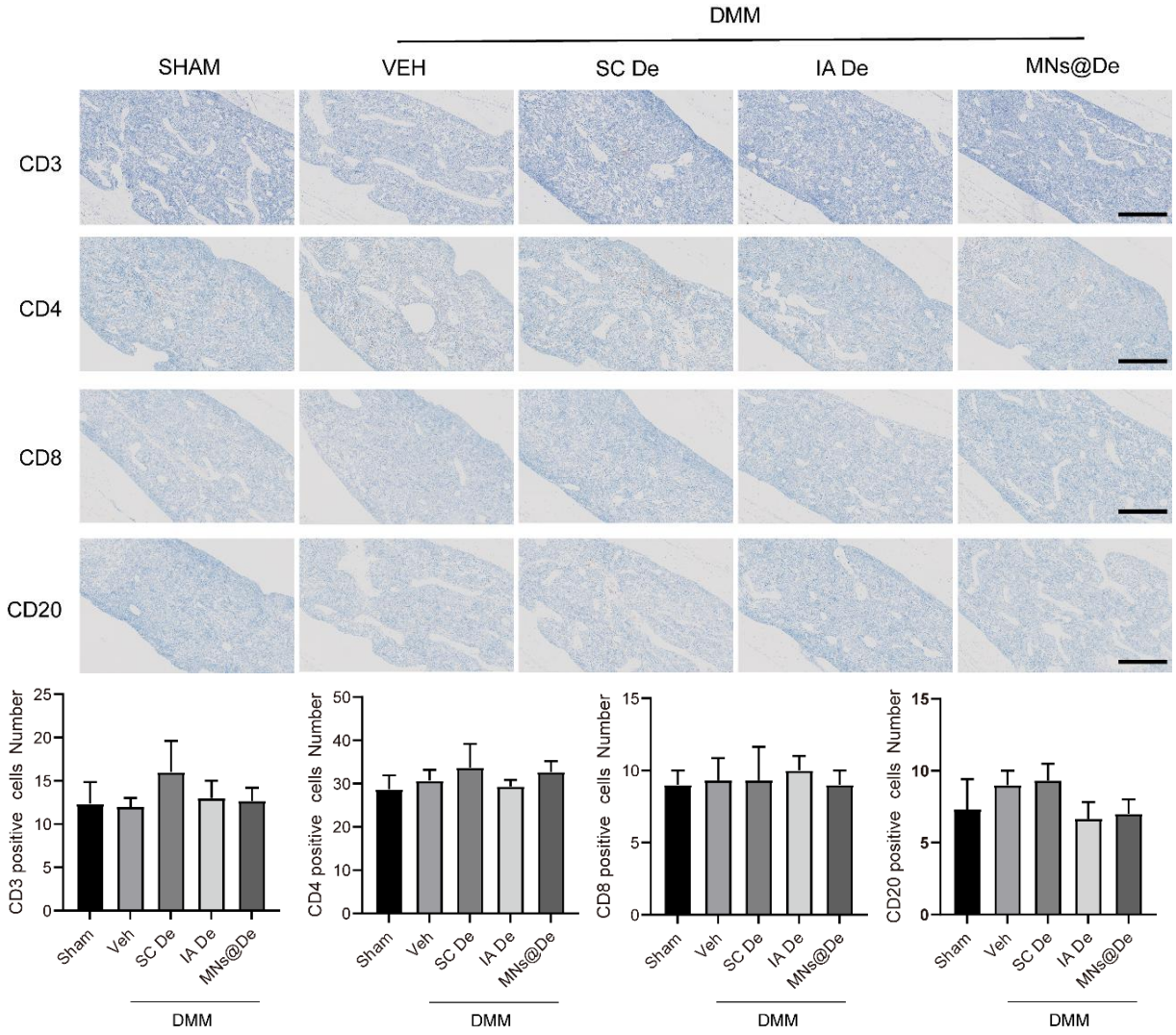


**Figure S5:** Immunohistochemical staining images and quantification for CD3, CD4, CD8 and CD20 in sham, DMM, SC De, IA De and MNs@De mice bone marrow; scale bar = 200 μm.

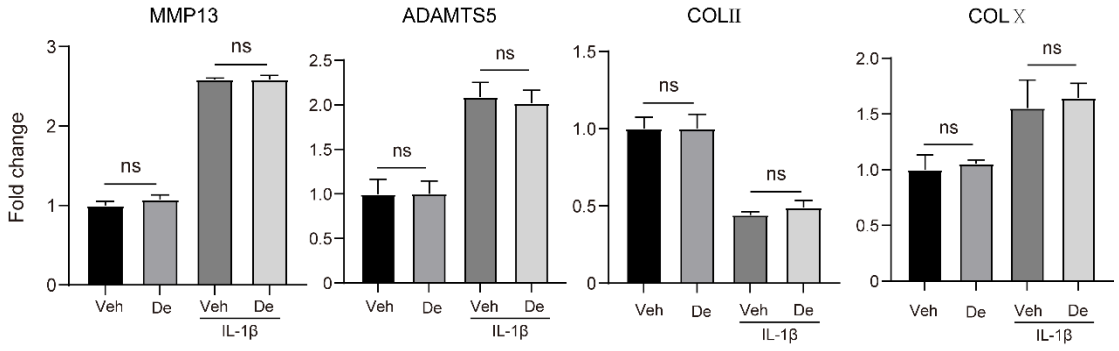


**Figure S6:** RT-qPCR was performed to assess the mRNA levels of MMP13,

ADAMTS5,COLII and COLX in chondrocyte from the Veh, De, IL-1β+veh, and IL-1β+De groups (n = 5 per group). Statistical analyses were conducted using one-way ANOVA followed by the by Dunnett multiple comparisons test. Error bars are mean ± SD, * $P < 0.05$, ** $P < 0.01$, *** $P < 0.001$, **** $P < 0.0001$.

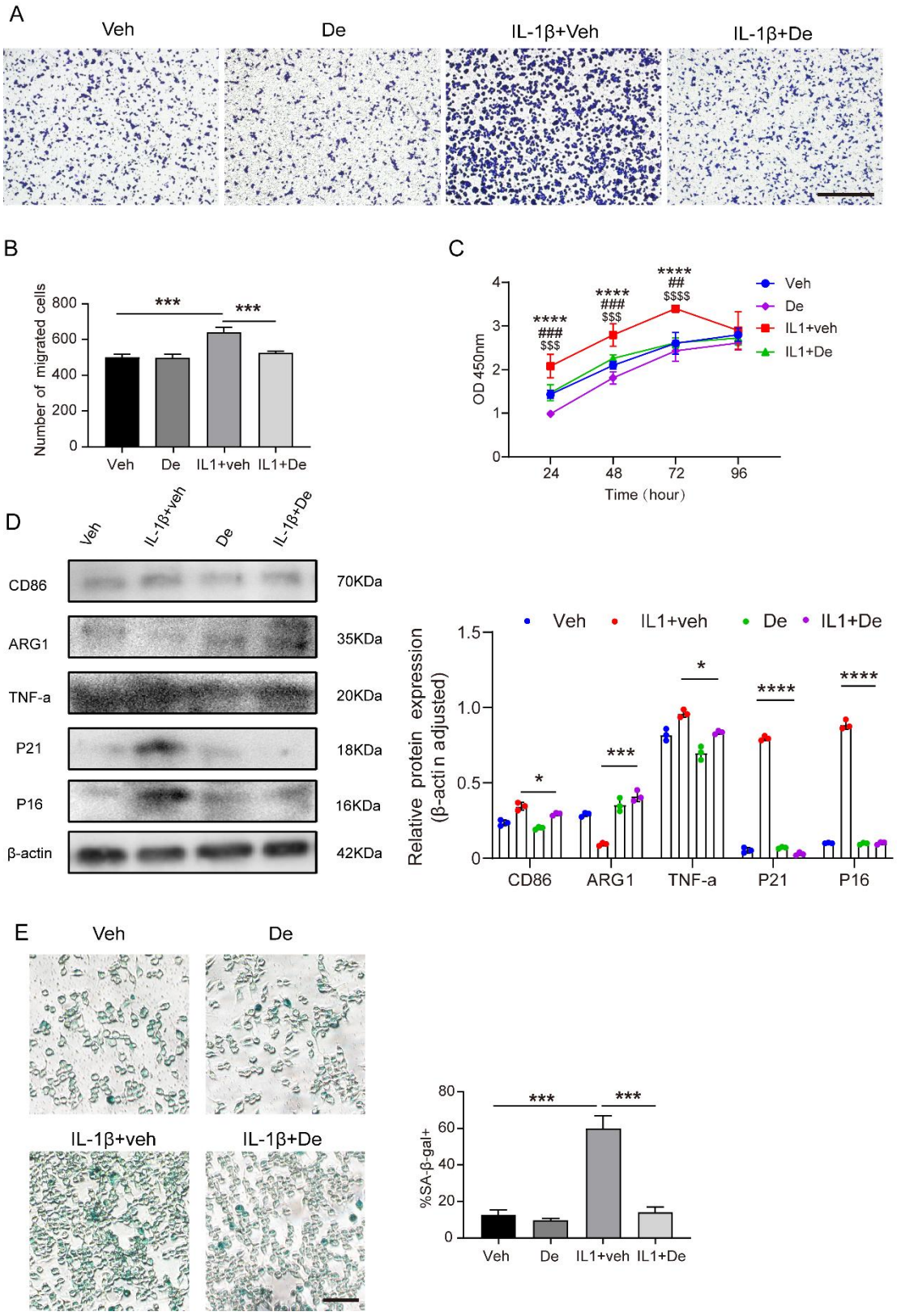


**Figure S7: Denosumab reduces macrophage migration and proliferation, and polarizes them towards the M2 phenotype.**

(A) Representative transwell migration assay of macrophages.

Macrophages were seeded on the upper chamber at 2,000 cells/mL, then IL-1β or denosumab was added to the lower chamber. After 12 hours, migrated cells on the lower surface of the Transwell™ membrane were stained with crystal violet. Scar bar,100um.(B) Semi-quantitative analysis of macrophage migration numbers. (n = 3 per group). (C) The CCK-8 assay measures absorbance at 450 nm to reflect the proliferation of macrophages.*,Veh vs IL-1β;#,IL-1β VS IL-1β+De;$,IL-1β+De vs De. (n = 5 per group). (D) Western blot analysis of CD86, TNF-a, ARG1,P16,P21in vehicle, IL-1 β , IL-1 β + De and De treated Macrophages(n = 3 per group).(E) SA-β-gal staining of macrophages induced to inflammation by IL-1β and semi-quantitative analysis,scar bar,200um.(n = 3 per group). Statistical analyses were conducted using one-way ANOVA followed by the by Dunnett multiple comparisons test.Error bars represent mean ± SD, * $P < 0.05$, **/##$P < 0.01$, ***/###/$$$$P<0.001$,****/$$$$$P < 0.0001$.

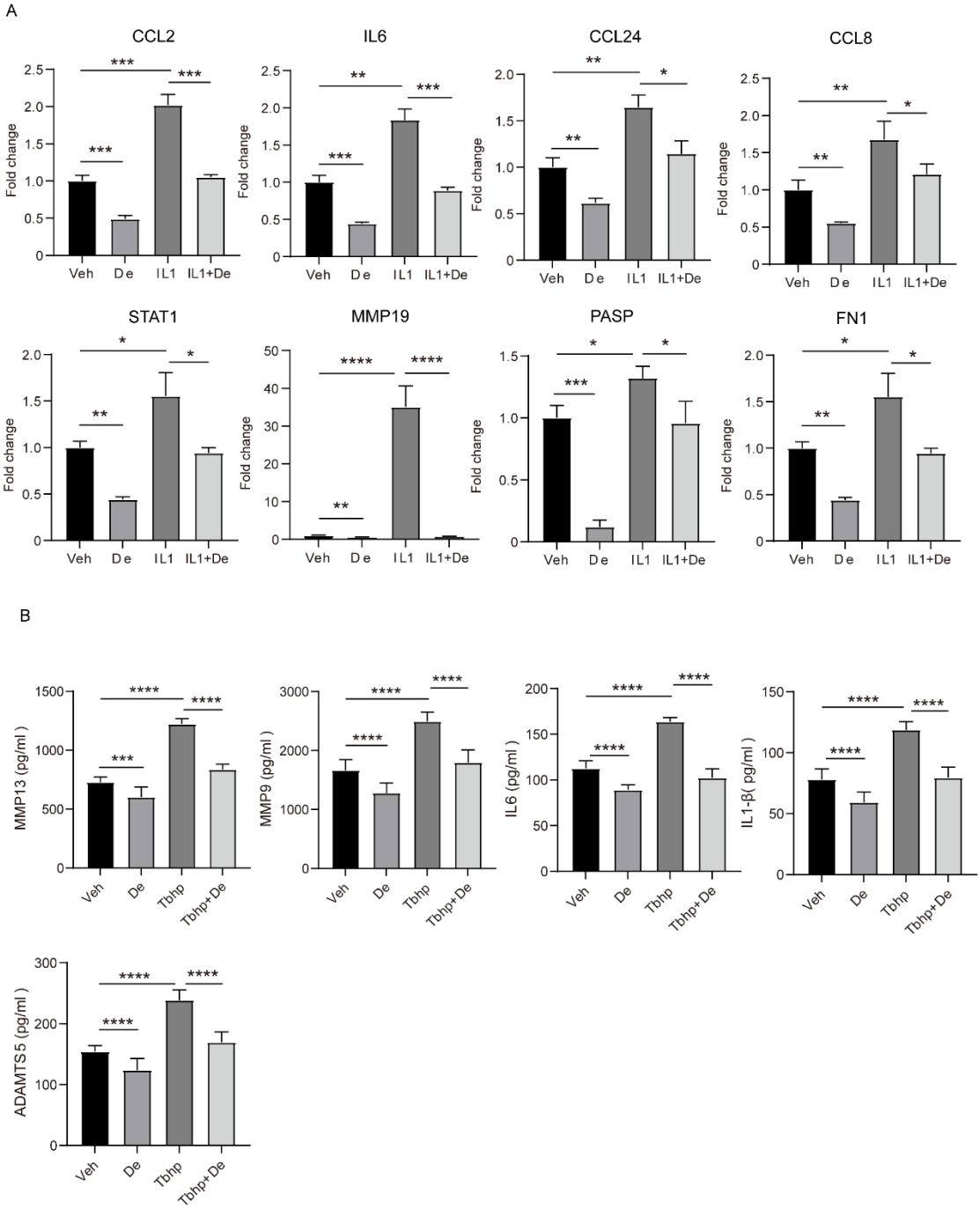


**Figure S8:** (A) RT-qPCR was performed to assess the mRNA levels of CCL2, CCL8, CCL24, IL6, STAT1, MMP19, PASP, and FN1 in macrophages from the Veh, De, IL-1β+veh, and IL-1β+De groups (n = 5 per group). (B) The concentrations of MMP13, MMP9, IL-6, IL-1β, and ADAMTS5 in macrophages from the Veh, De, Tbhp, and Tbhp+De groups were assessed by enzyme-linked immunosorbent assay (n = 8 per group).

Statistical analyses were conducted using one-way ANOVA followed by the by Dunnett multiple comparisons test. Error bars are mean ± SD, * $P < 0.05$, ** $P < 0.01$, *** $P < 0.001$, **** $P < 0.0001$.

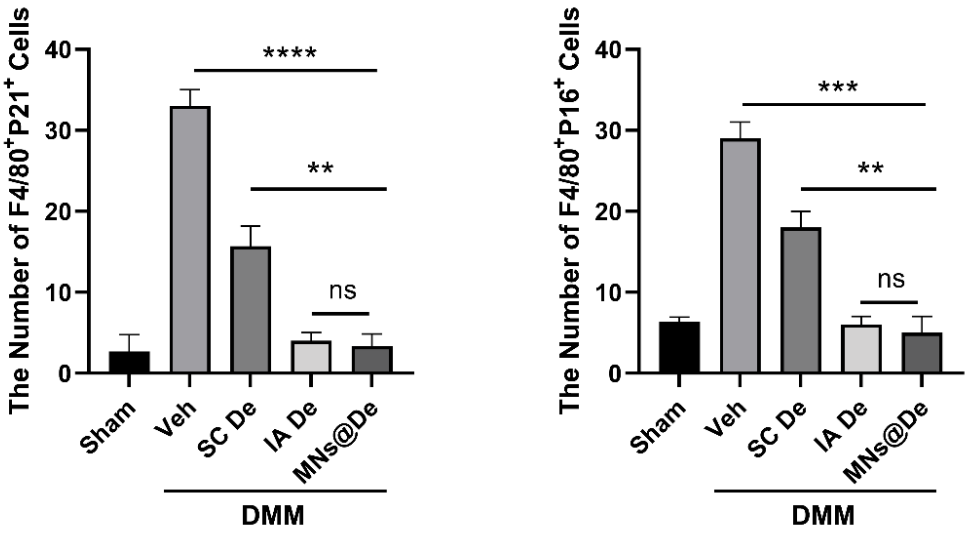


**Figure S9:** quantification of P16/P21-positive cells in synovial tissues from mice in the Sham, DMM+Veh, DMM+SC De, DMM+IA De, and DMM+MNs@De groups.(n=5) Statistical analyses were conducted using one-way ANOVA followed by the by Dunnett multiple comparisons test. Error bars are mean ± SD, * $P < 0.05$, ** $P < 0.01$, *** $P < 0.001$, **** $P < 0.0001$.

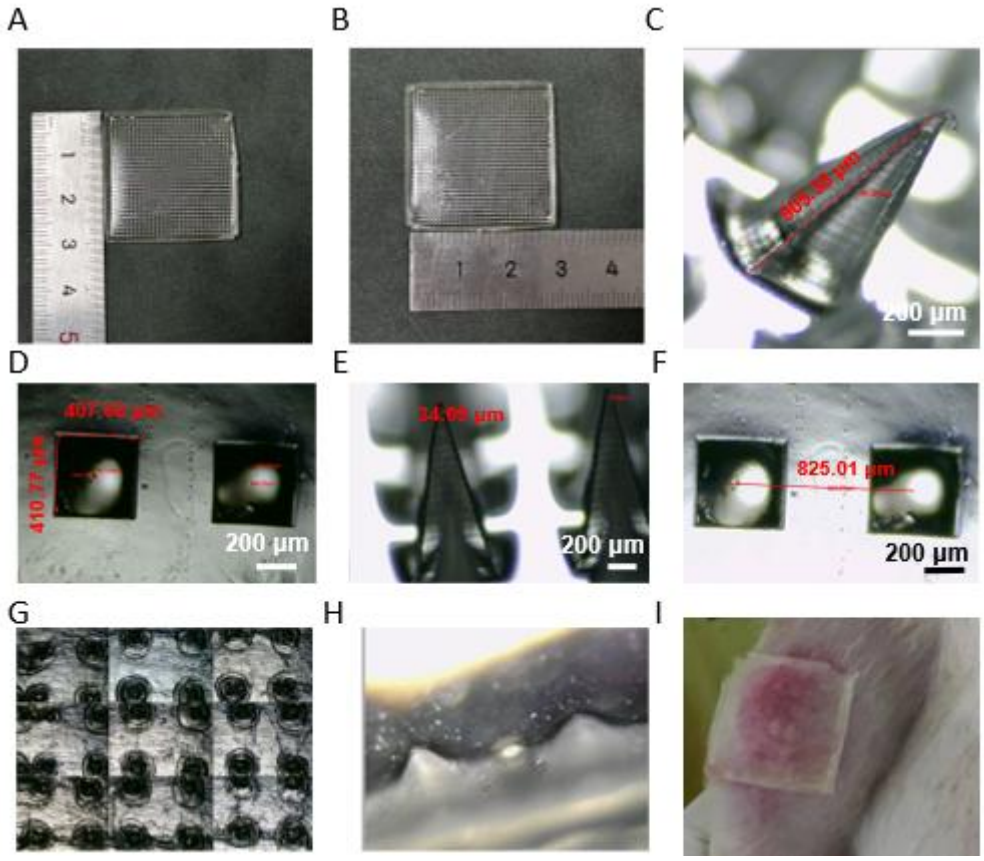


**Figure S10: Characterization of MN patch for large animal (dog) Applications.**

(A ,B) Dimensional analysis of MN patch length and width (3 cm × 3 cm). (C) Morphological characterization and height measurement of microneedle tips (805-905 µm). (D) Quantitative assessment of base dimensions (404-435 µm) and (E) Tip apex width for individual MN measurement (30-44 µm). (F) Inter-needle spacing analysis between adjacent MN (819-844 µm). (G) Penetration capability evaluation through the five-layer parafilm M barriers of MN. (H) In vitro dissolution of MN patch in aqueous medium. (I) Photograph of MN patch application on the dog joint anatomy.

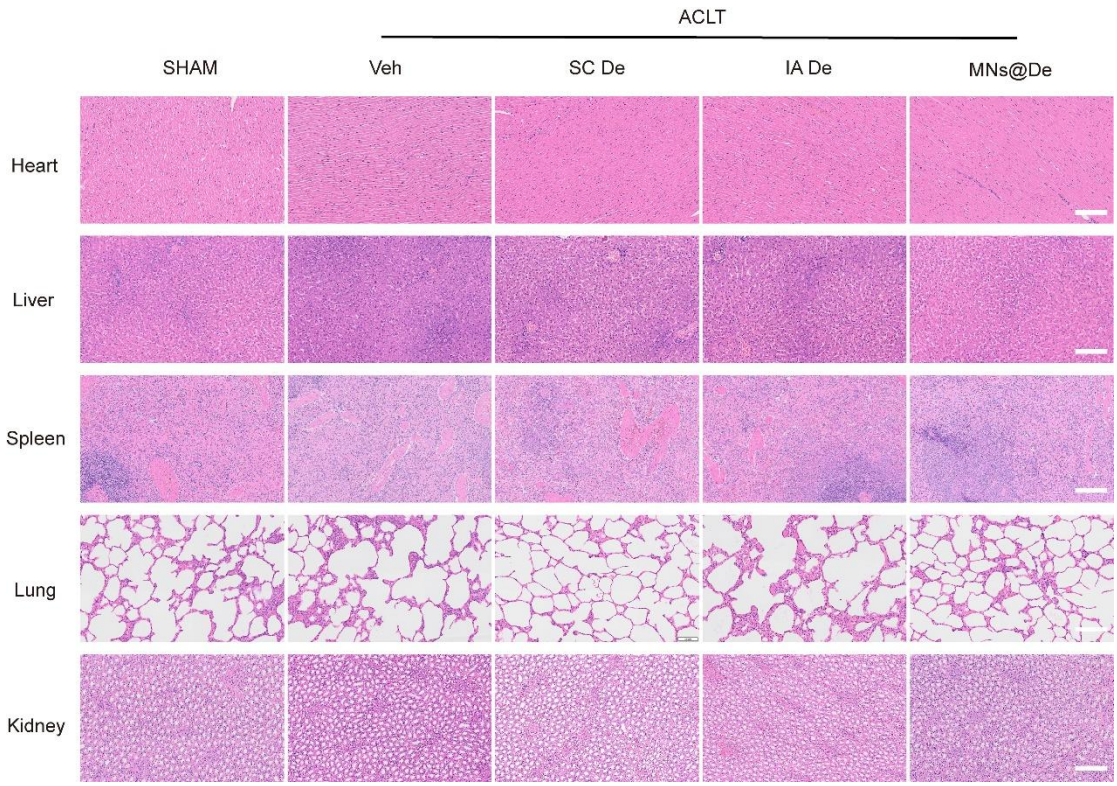


**Figure S11: Microneedle toxicity testing on major organs of beagles.**

H&E staining of organs (heart, liver, spleen, lung, kidney) in SHAM, ACLT, SC De, IA De and MNs@De beagles. Scar bar, 100um